Poisson's ratio in layered two-dimensional crystals

Sungjong Woo,[1] Hee Chul Park,[1,2] and Young-Woo Son[1]
[1]*Korea Institute for Advanced Study, Seoul 130-722, Republic of Korea*
[2]*Center for Theoretical Physics of Complex Systems, Institute of Basic Science, Daejeon 34051, Republic of Korea*
(Received 1 June 2015; revised manuscript received 2 January 2016; published 11 February 2016)

We present first-principles calculations of elastic properties of multilayered two-dimensional crystals, such as graphene, h-BN, and $2H$-MoS_2, which show that their Poisson's ratios along the out-of-plane direction are negative, near zero, and positive, respectively, spanning all possibilities for the sign of the ratios. While the in-plane Poisson's ratios are all positive regardless of their disparate electronic and structural properties, the characteristic interlayer interactions as well as layer stacking structures are shown to determine the sign of their out-of-plane ratios. A thorough investigation of elastic properties as a function of the number of layers for each system is also provided, highlighting their intertwined nature between elastic and electronic properties.

DOI: 10.1103/PhysRevB.93.075420

I. INTRODUCTION

Under uniaxial stress, Poisson's ratio defined by the ratio of the strain in the transverse direction, ϵ_t, to that of the longitudinal direction, ϵ_l, $\nu = -\epsilon_t/\epsilon_l$, measures the fundamental mechanical responses of solids against external loads [1–5]. It has a strong correlation with the atomic packing density, atomic connectivity [2], and structural phase transition [3–5]. The theory of elasticity allows values of Poisson's ratio of an isotropic material ranging from -1 to 0.5, i.e., from extremely compressible to incompressible materials [1,5]. Thus, when a solid is subjected to a uniaxial compression, it expands ($\nu > 0$), remains the same ($\nu = 0$), or shrinks ($\nu < 0$) in the transverse direction depending on the sign of Poisson's ratio. Typically, different Poisson's ratios or their signs indicate dramatic variations in mechanical properties. For example, when the isothermal modulus is extremely larger than the shear modulus, the material reaches its incompressible limit as shown in most liquids or rubber ($\nu \sim 0.5$), and in the opposite case, reentrant foams and related structures show the negative ν or auxetic property [5–9]. Poisson's ratio of common solid state crystals usually falls in the range of $0 < \nu < 0.5$ while gases and cork have $\nu \simeq 0$ [5–9].

Anisotropic materials with directional elastic properties often show more dramatic variations in their Poisson's ratios such as the directional auxetic property [5]. In this regard, the experimental realization of graphene [10,11], the thinnest and the strongest material [12–15], now offers a new platform to understand electronic and elastic properties of well-defined anisotropic materials and their heterostructures. Even though Young's modulus and Poisson's ratio of graphene have been studied quite thoroughly [12–22], those along the out-of-plane direction for its few-layered forms have barely been known. Neither do all the other available two-dimensional crystals. Since electronic properties of layered two-dimensional crystals vary a lot depending on their chemical composition as well as the number of layers [23–25], their corresponding elastic properties, especially for few-layered structures, are anticipated to change accordingly. Motivated by recent rapid progress in manipulating various two-dimensional crystals and their stacking structures [24–26], we have calculated fundamental mechanical properties of three representative van der Waals (vdW) crystals along all crystallographic directions of their few-layered structures.

In this article, we present a theoretical study using a first-principles approach on the elastic properties of layered two-dimensional crystals, including graphene, h-BN, and $2H$-MoS_2, in which the vdW energy is one of the governing interactions between their layers while they exhibit very different electronic properties. We find that the Poisson's ratios of graphene, h-BN, and $2H$-MoS_2 along out-of-plane direction are negative, near zero, and positive, respectively, whereas their in-plane Poisson's ratios are all positive. The diverseness of out-of-plane Poisson's ratio is attributed to their disparate electronic properties as well as stacking structures. Thorough investigation on their elastic properties while varying the number of layers are also reported.

II. COMPUTATIONAL DETAILS

We first consider graphene with AB stacking, h-BN, and $2H$-MoS_2 with AA' stacking. All three have C_{3v} symmetry. Generally, for a material with C_{3v} symmetry, the stiffness tensor without a shear part can be written with four independent parameters,

$$\begin{pmatrix}\sigma_x\\ \sigma_y\\ \sigma_z\end{pmatrix} = \begin{pmatrix}A & B & C\\ B & A & C\\ C & C & D\end{pmatrix}\begin{pmatrix}\epsilon_x\\ \epsilon_y\\ \epsilon_z\end{pmatrix}, \tag{1}$$

with the choice of z as the axis for the three-fold rotational symmetry [1]. Here, σ_i and ϵ_i are the stress and strain, respectively, along the ith axis. The components of the stiffness tensor can be obtained by differentiating the total energy $E_{\rm tot}$ in terms of strain: $A = \partial^2 E_{\rm tot}/\partial\epsilon_x^2 = \partial^2 E_{\rm tot}/\partial\epsilon_y^2$, $B = \partial^2 E_{\rm tot}/\partial\epsilon_x\partial\epsilon_y$, $C = \partial^2 E_{\rm tot}/\partial\epsilon_x\partial\epsilon_z$, and $D = \partial^2 E_{\rm tot}/\partial\epsilon_z^2$. By taking the inverse of the stiffness tensor, one can get the compliance tensor,

$$\begin{pmatrix}\epsilon_x\\ \epsilon_y\\ \epsilon_z\end{pmatrix} = \begin{pmatrix}1/E_i & -\nu_i/E_i & -\tilde{\nu}_o/E_o\\ -\nu_i/E_i & 1/E_i & -\tilde{\nu}_o/E_o\\ -\nu_o/E_i & -\nu_o/E_i & 1/E_o\end{pmatrix}\begin{pmatrix}\sigma_x\\ \sigma_y\\ \sigma_z\end{pmatrix}. \tag{2}$$

The subscripts i and o represent *in-plane* and *out-of-plane*, respectively. E_i and E_o are Young's moduli along the $x(y)$ and z axes, respectively. There are two out-of-plane Poisson's ratios: ν_o is the Poisson's ratio along the z axis when the stress is

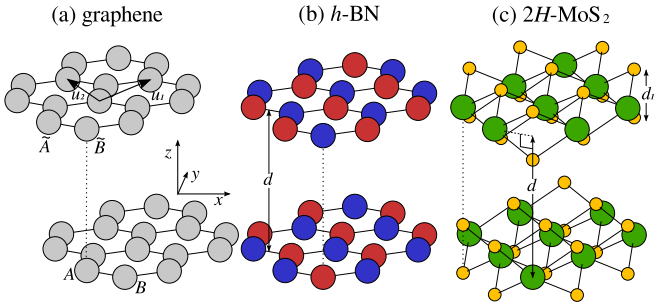

FIG. 1. Lattice structures of (a) AB-stacked graphene, (b) AA'-stacked h-BN where red and blue circles denote boron and nitrogen atoms respectively, and (c) $2H$-MoS_2. The parameter d is the interlayer distance of each structure. In $2H$-MoS_2, d is the vertical distance between Mo atoms in adjacent layers, and d_1 is the vertical intralayer sulfur-to-sulfur distance.

applied along the x or y direction while $\tilde{\nu}_o = \nu_0 E_0/E_i$ is the Poisson's ratio along the x or y direction when the stress is applied along the z direction. ν_i is the in-plane Poisson's ratio along the $x(y)$ axis when the stress is applied along the $y(x)$ axis.

Using a first-principles approach based on density-functional theory with a plane wave basis set [27], we calculate total energies $E_{\rm tot}(\epsilon_x,\epsilon_y,\epsilon_z)$ of all systems at $5 \times 5 \times 5$ grid points in the strain space of $(\epsilon_x,\epsilon_y,\epsilon_z)$. Strains are applied by modifying the unit cell vectors. To obtain the accurate binding energy and interlayer distance including the vdW energy, we have used the revised version [28] of the nonlocal correlation functional method developed by Vydrov and van Voorhis [29] that is successful for reproducing both values following results from more accurate methods [30]. In order to reduce spurious interaction between neighboring supercells, a large vacuum over 68 Å is introduced and relatively high energy cutoff above 100 Ry as well as dense k-point grids up to 29×29 are used to converge the results.

For the total energy calculations with tensile strain on all systems in which the layers are stacked along the z axis, a primitive cell with unit vectors, $u_1 = (a,b,0)$, $u_2 = (-a,b,0)$, $u_3 = (0,0,c)$, are used (Fig. 1). Strain along the x and y axes is defined by $\epsilon_x = (a - a_0)/a_0$ and $\epsilon_y = (b - b_0)/b_0$, where a_0 and b_0 are the lattice parameters of the equilibrium structure. Strain across the layers along the z axis is defined by $\epsilon_z = (d - d_0)/d_0$ where d and d_0 are the interlayer distance and that of the equilibrium structure, respectively. The calculated lattice parameters of a_0 and d_0 for infinitely stacked bulk systems are 2.47, 2.52, 3.22 Å and 6.72, 6.61, 12.42 Å for graphite, h-BN, and $2H$-MoS_2, respectively, which are in excellent agreements with previous studies [31–34]. The slight variation of a_0, b_0, and d_0 depending on the number of layers are reflected in our calculations. A, B, C, and D in Eq. (1) are calculated by interpolating $E_{\rm tot}$ on the strain space and Young's modulus and Poisson's ratio from the compliance tensor in Eq. (2).

III. RESULTS AND DISCUSSION

Figure 2 shows Young's moduli and Poisson's ratios for the three materials with various numbers of layers. In-plane elastic constants, E_i and ν_i, are barely dependent on the number of

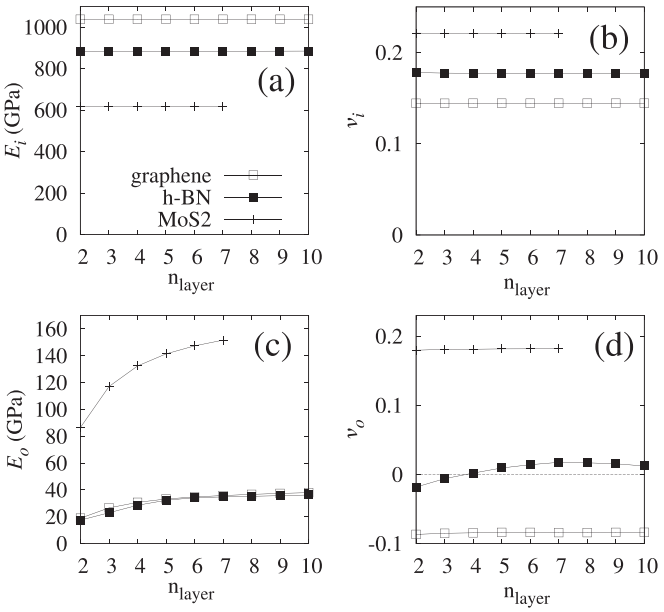

FIG. 2. Elasticity constants of graphene (empty rectangles), h-BN (filled rectangles), and $2H$-MoS_2 (crosses) as a function of the number of layers up to ten layers: in-plane (a) Young's moduli and (b) Poisson's ratios and out-of-plane (c) Young's moduli and (d) Poisson's ratios.

layers [Figs. 2(a) and 2(b)]. Under in-plane tensile stress, the hexagonal network of atoms is deformed for graphene and h-BN while, for $2H$-MoS_2, sulfur-to-sulfur distance across the plane along the z axis within one layer can also be deformed. Furthermore, the hexagonal structure of graphene and h-BN with rigid σ bonds supported by π bonds is stiffer than that of $2H$-MoS_2. This makes $2H$-MoS_2 more flexible to applied stress resulting in a lower in-plane Young's modulus [Fig. 2(a)] and a larger in-plane Poisson's ratio [Fig. 2(b)]. Young's moduli across layers, E_o, increase for all of the three materials with the increase of the number of layers reflecting the accumulation of long-range interlayer van der Waals interaction [Fig. 2(c)].

Contrary to similar behaviors between in-plane elastic properties of the three materials, out-of-plane elastic properties between those differ qualitatively [Fig. 2(d)]. The most notable one is that multilayered graphene structures have out-of-plane Poisson's ratios as negative as $\nu = -0.09$ [Fig. 2(d)] with a slight dependence on the layer number variations. Materials with axial negative Poisson's ratios have been reported during the last few decades, such as foams with reentrant atomic structures [5–9] and those with nonaxial ones are shown in some simple cubic metals [35,36]. The present case is for the axial negative ratio in a layered material where the vdW interaction governs the binding between layers without reentrant structure. More interestingly, h-BN shows a very small out-of-plane Poisson's ratio near zero crossing from negative to positive values as the number of layers increases whereas $2H$-MoS_2 has a positive Poisson's ratio as shown in Fig. 2(d). So, the three layered crystals have qualitatively different Poisson's ratios spanning all possibilities of their signs.

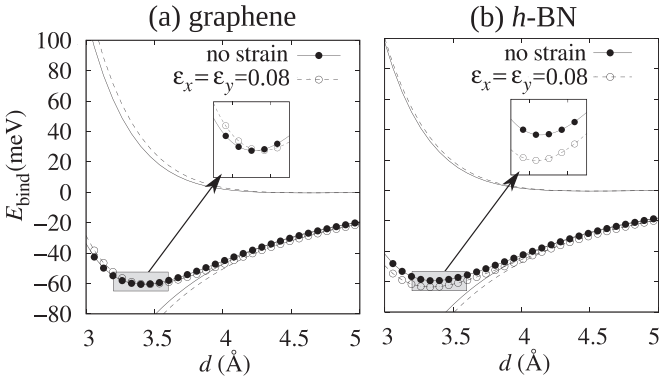

FIG. 3. Binding energy as a function of interlayer distance d for bilayer (a) graphene and (b) h-BN. The fitting curves for the attractive and repulsive parts are drawn in for the unstrained case (solid line) and $\epsilon_x = \epsilon_y = 0.08$ equibiaxial strain case (dashed line). The insets show magnified views near equilibrium.

A. Pauli repulsion vs vdW attraction

To understand the qualitative difference in out-of-plane Poisson's ratios of the three layered systems, we first decompose the binding energy of bilayer systems into repulsive and attractive parts. Figure 3(a) shows the binding energy curve between two layers of graphene, $E_{\rm bind}(d) \equiv \frac{1}{2}[E^{\rm b}_{\rm tot}(d) - 2E^{\rm s}_{\rm tot}]$ where $E^{\rm b(s)}_{\rm tot}$ is the total energy of bilayer (single layer) graphene. $E_{\rm bind}(d)$ is shown as solid (no strain) and open (8.1% equibiaxial nominal strain) circles as a function of the distance d between the layers. The calculated binding energy within $d = 4$ to 9 Å is well described by $E_{\rm bind}(d) \sim d^{-4}$. The fitting curve of d^{-4}, which reflects asymptotic vdW interaction [37], is drawn in as a solid (dashed) line without (with) strain. The difference between the total energy and vdW energy for each case is also plotted in the same plot, two curves on top, representing purely repulsive characteristics called Pauli repulsion [38,39]. It does not fit to any single power of $d^{-\alpha}$ but is well fit by an exponentially decaying function, $E_{\rm bind}(d) \sim [\exp(d^2/\sigma^2) - 1]^{-1}$, with $\sigma = 1.37$ Å for the case without strain. We note that the d^{-3} dependence of the vdW energy of bilayer graphene, which was recently reported [40], is valid only at a distance larger than 9 Å [41]; therefore it is not relevant near the equilibrium distance considered here.

Figure 3(a) indicates that both vdW attraction and Pauli repulsion on bilayer graphene are enhanced under tensile strain. However, noting that the Pauli repulsion energy showing an exponential increase with d is much stiffer than the attractive vdW energy, equilibrium interlayer distance is critically sensitive to the change of the former rather than the latter. Thus, the equilibrium interlayer distance under the strain is mainly determined not by the strain-enhanced vdW attraction [42] but by the enhancement of the repulsion. In graphene, electronic states pointing away from the layers are composed of linear combinations of p_z orbitals of atoms called π orbitals and form the π band [43]. Since the occupied electrons of π orbitals in adjacent layers expel each other from their overlap region [44], the enhanced repulsion with external strain shown in Fig. 3(a) may indicate the strain-induced spatial variation of π electrons pushing the two layers away while the vdW interaction still keeps their binding.

B. Elongation of π band orbitals

We find that the in-plane strain indeed elongates the spatial distribution of electron density away from the layer making the Pauli repulsion increase over the vdW attraction. We calculate the spatial distribution of density of the π band along the z axis in a single layer graphene; $\rho_\pi(z) \equiv \int_{-\infty}^{\varepsilon_F} dE \int dx dy \rho_E(x,y,z)$. Here, $\rho_E(x,y,z)$ is the local density of state for the π band only and is summed over the in-plane unit cell (x and y axis). Graphene is located at $z = 0$ and the Fermi energy of the neutral system is denoted by ε_F. Our *ab initio* calculation result for the maximum of $\rho_\pi(z)$ decreases with tensile strain while its tail increases implying that π orbital spreads out along the z axis with strain. Quantitatively, we calculate the density-weighted length of π orbital along the z axis using $L_\pi \equiv \int dz|z|\rho_\pi(z)/\int dz\rho_\pi(z)$ that gives $L_\pi = 0.673$ Å without strain. We find that the value of L_π indeed increases by 0.6% as the equibiaxial strain increases by 2%, thereby explaining the value of the negative Poisson's ratio near -0.1 along out-of-plane direction. This elongation can be understood simply by considering overlaps between neighboring atomic orbitals. For a charge neutral graphene, the spatial distribution of π orbitals along the perpendicular direction to the layer is contracted compared to p_z orbitals of an isolated carbon atom because of overlap between nearby p_z orbitals. In-plane tensile strain returns the carbon atoms in graphene back to isolated one so that the π orbitals should be elongated.

A simple tight-binding (TB) picture can corroborate the elongation of spatial distribution of π orbitals under strain. Consider the Bloch wave function within the TB approximation, $\phi_{A(B)}(\vec{k},\vec{r}) = N^{-1/2}\sum_{\vec{R}_{A(B)}} e^{i\vec{k}\cdot\vec{R}_{A(B)}}\varphi_{A(B)}(\vec{r} - \vec{R}_{A(B)})$, where subscript $A(B)$ represents the sublattice index, $\varphi_{A(B)}(\vec{r} - \vec{R}_{A(B)})$ is the normalized p_z orbital of the carbon atom at $\vec{R}_{A(B)}$, while $\vec{R}_{A(B)}$ runs the positions of atoms in the $A(B)$ sublattice [43]. With the nearest neighbor hopping t and the overlap, $s = \langle\varphi_A(\vec{r} - \vec{R}_A)|\varphi_B(\vec{r} - \vec{R}_A - \vec{\delta}_j)\rangle$, the π orbital is given by $\psi_\pi(\vec{k},\vec{r}) = \frac{f(\vec{k})}{|f(\vec{k})|}\phi_A(\vec{k},\vec{r}) + \phi_B(\vec{k},\vec{r})$ where $f(\vec{k}) = \sum_{j=1}^{3} e^{i\vec{k}\cdot\vec{\delta}_j}$ and $\vec{\delta}_j$ points to the three nearest neighbors. Considering $s \ll 1$, $L_\pi = \frac{1}{S_{\rm BZ}}\int_{\rm BZ} d^2k l_\pi(\vec{k})$, where $l_\pi(\vec{k}) \equiv \frac{\langle\psi_\pi(\vec{k})||z||\psi_\pi(\vec{k})\rangle}{\langle\psi_\pi(\vec{k})|\psi_\pi(\vec{k})\rangle} \approx l_{p_z} - |f(\vec{k})|(l_{p_z}s - l_\delta)$ is the density-weighted length of the π orbital at $\vec{k}$ and $S_{\rm BZ}$ is the area of the first Brillouin zone (BZ). Here, $l_{p_z} = \int d^3r|z||\varphi_A(\vec{r})|^2$ is the length of an isolated p_z orbital and $l_\delta = \int d^3r\varphi^*_A(\vec{r} - \vec{R}_A)|z|\varphi_B(\vec{r} - \vec{R}_A - \vec{\delta}_1)$. If the maximum overlap between nearest neighbor p_z orbitals is at $|z| = z_0$ and $\varphi^*_A(\vec{r} - \vec{R}_A)\varphi_B(\vec{r} - \vec{R}_A - \vec{\delta}_1)$ is trivial elsewhere, then $l_\delta \approx z_0 s$ so that $l_\pi(\vec{k}) \approx l_{p_z} - |f(\vec{k})|(l_{p_z} - z_0)s$ and that $L_\pi \approx l_{p_z} - l_h(|\vec{\delta}_1|)$ where $l_h \equiv \frac{(l_{p_z} - z_0)s}{S_{\rm BZ}}\int_{\rm BZ} d^2k|f(\vec{k})|$. It is straightforward to find that $l_h > 0$ and $\partial l_h/\partial|\vec{\delta}_1| < 0$. Therefore, the above simple formulation for L_π implies that the out-of-plane distance of π orbital is shorter than that of bare p_z orbital and that the applied tensile strain can increase its distance.

C. Graphene, h-BN, and MoS_2

Now, let us compare elastic properties of multilayered h-BN with graphene. A previous study [45] shows that the ionic

interaction energy in the h-BN is negligible in determining the electrostatic repulsion as well as dispersion forces so that the interlayer distance is very similar to graphite regardless of the apparent difference in the static polarizability between the two layered materials. Our analysis, however, shows the elastic properties can be quite different; the amplitude of the out-of-plane Poisson's ratio of h-BN is nowhere close to that of multilayer graphene but is an order of magnitude smaller than that of multilayer graphene [Fig. 2(d)]. Figure 3(b) shows that under tensile strain, the vdW interaction increases as in graphene while the Pauli repulsion barely changes. For a bilayer graphene with AB stacking, half of the carbon atoms of one layer are right on top of the carbon atoms of the other layer so that the tails of p_z orbitals from two layers directly overlap with each other. For a bilayer h-BN with AA' stacking, however, fully filled p_z orbital of the nitrogen atom from one layer is on top of the empty p_z orbital of boron from the other layer so that the interlayer Pauli repulsion is not as sensitive to the slight change of the length of p_z orbitals as in the case of graphene.

The length of p_z orbital of a single-layer h-BN, in fact, does change due to the strain in the same manner as that of graphene. Therefore, a negative interlayer Poisson's ratio should appear in h-BN as multilayer graphene if the interlayer alignment of p_z orbitals follows that of graphene. This can be realized by changing the stacking structure of h-BN from AA' to AA. We have computed the elastic properties for this artificial bilayer structure and found that the out-of-plane Poisson ratio is -0.12, thus confirming our theory. On the other hand, the out-of-plane Poisson's ratio of bilayer $2H$-MoS_2 is mainly determined by the flattening of each layer under tensile strain that gives positive value. Our calculation shows that the change of interlayer distance d of $2H$-MoS_2 in Fig. 1(c) in response to a given in-plane tensile stress mainly comes from the change of d_1; $\Delta d_1 \approx (3/4)\Delta d$.

IV. CONCLUSION

In conclusion, we have studied the elastic properties of multilayered two-dimensional crystals including graphene, h-BN, and $2H$-MoS_2, with interlayer van der Waals interaction properly taken into account. In-plane elastic properties are found to be barely dependent on the number of layers for all three materials. Our analysis reveals that graphene is a very peculiar axial auxetic material when in-plane strain is applied. The mechanism is attributed to a quantum mechanical origin rather than to a structural one such as reentrant foam. In contrast, the Poisson's ratio of h-BN with AA' stacking is found to be nearly zero and that of MoS_2 is positive.

ACKNOWLEDGMENTS

We thank Jae-Hyun Kim and Yun Hwangbo for fruitful discussions at an early stage of this study. Y.-W.S. was supported by the NRF funded by the MSIP of the Korean government (CASE, No. 2011-0031640; and QMMRC, No. R11-2008-053-01002-0). Computations were supported by the Center for Advanced Computation of Korea Institute for Advanced Study.

[1] L. D. Landau and E. M. Lifshitz, *Theory of Elasticity*, 3rd ed. (Butterworth-Heinemann, Oxford, 1986).
[2] R. A. Rouxel, J. Am. Ceram. Soc. **90**, 3019 (2007).
[3] P. H. Poole, T. Grande, C. A. Angell, and P. F. McMillan, Science **275**, 322 (1997).
[4] G. N. Greaves *et al.*, Science **322**, 566 (2008).
[5] G. N. Greaves, A. L. Greer, R. S. Lakes, and T. Rouxel, Nat. Mater. **10**, 823 (2011) and references therein.
[6] R. S. Lakes, Science **235**, 1038 (1987).
[7] B. D. Caddock and K. E. Evans, J. Phys. D **22**, 1877 (1989).
[8] G. Milton, J. Mech. Phys. Solids **40**, 1105 (1992).
[9] K. E. Evans, M. A. Nkansah, I. J. Hutchinson, and S. C. Rogers, Nature (London) **353**, 124 (1991).
[10] K. S. Novoselov *et al.*, Science **306**, 666 (2004).
[11] Y. Zhang, Y.-W. Tan, H. L. Stormer, and P. Kim, Nature (London) **438**, 201 (2005).
[12] C. Lee, X. Wei, J. W. Kysar, and J. Hone, Science **321**, 385 (2008).
[13] C. A. Marianetti and H. G. Yevick, Phys. Rev. Lett. **105**, 245502 (2010).
[14] C. Si, W. Duan, Z. Liu, and F. Liu, Phys. Rev. Lett. **109**, 226802 (2012).
[15] S. J. Woo and Y.-W. Son, Phys. Rev. B **87**, 075419 (2013).
[16] S. P. Koenig, N. G. Boddeti, M. L. Dunn, and J. S. Bunch, Nanotech. **6**, 543 (2011).
[17] Y. Y. Zhang and Y. T. Gu, Comput. Mater. Sci. **71**, 197 (2013).
[18] S. A. H. Kordkheili and H. Moshrefzadeh-Sani, Comput. Mater. Sci. **69**, 335 (2013).
[19] O. L. Blakslee, D. G. Proctor, E. J. Seldin, G. B. Spence, and T. Weng, J. Appl. Phys. **41**, 3373 (1970).
[20] A. Politano, A. R. Marino, D. Campi, D. Farías, R. Mirandac, and G. Chiarello, Carbon **50**, 4903 (2012).
[21] F. Scarpa, S. Adhikari, and A. S. Phani, Nanotech. **20**, 065709 (2009).
[22] M. Liu and F. Liu, Nanotech. **25**, 135706 (2014).
[23] K. S. Novoselov *et al.*, Proc. Natl. Acad. Sci. USA **102**, 10451 (2005).
[24] A. K. Geim and K. S. Novoselov, Nat. Mater. **6**, 183 (2007).
[25] A. K. Geim and I. V. Grigorieva, Nature (London) **499**, 419 (2013).
[26] C. Dean *et al.*, Sol. Stat. Commun. **152**, 1275 (2012).
[27] P. Ginannozzi *et al.*, J. Phys. Condens. Matter **21**, 395502 (2009).
[28] R. Sabatini, T. Gorni, and S. de Gironcoli, Phys. Rev. B **87**, 041108(R) (2013).
[29] O. A. Vydrov and T. van Voorhis, J. Chem. Phys. **133**, 244103 (2010).
[30] T. Björkman, A. Gulans, A. V. Krasheninnikov, and R. M. Nieminen, Phys. Rev. Lett. **108**, 235502 (2012).
[31] Y. Baskin and L. Meyer, Phys. Rev. **100**, 544 (1955).
[32] W. Paszkowicz, J. B. Pelka, M. Knapp, T. Szyszko, and S. Podsiadlo, Appl. Phys. A **75**, 431 (2002).

[33] R. G. Dickinson and L. Pauling, J. Am. Chem. Soc. **45**, 1466 (1923).
[34] F. Jellinek, G. Brauer, and H. Müller, Nature (London) **185**, 376 (1960).
[35] F. Milstein and K. Huang, Phys. Rev. B **19**, 2030 (1979).
[36] R. H. Baughman, J. M. Shacklette, A. A. Zakhidov, and S. Stafström, Nature (London) **392**, 362 (1998).
[37] H. Rydberg, M. Dion, N. Jacobson, E. Schröder, P. Hyldgaard, S. I. Simak, D. C. Langreth, and B. I. Lundqvist, Phys. Rev. Lett. **91**, 126402 (2003).
[38] J. H. Jensen and M. S. Gordon, Mol. Phys. **89**, 1313 (1996).
[39] O. V. Gritsenko, P. R. T. Schipper, and E. J. Baerends, Phys. Rev. A **57**, 3450 (1998).
[40] J. F. Dobson, A. White, and A. Rubio, Phys. Rev. Lett. **96**, 073201 (2006).
[41] S. Lebègue, J. Harl, T. Gould, J. G. Ángyán, G. Kresse, and J. F. Dobson, Phys. Rev. Lett. **105**, 196401 (2010).
[42] A. Sharma, P. Harnish, A. Sylvester, V. N. Kotov, and A. H. Castro Neto, Phys. Rev. B **89**, 235425 (2014).
[43] R. Saito, G. Dresselhaus, and M. S. Dresselhaus, *Physical Properties of Carbon Nanotubes* (Imperial College Press, London, 1998).
[44] J. Berashevich and T. Chakraborty, Phys. Rev. B **84**, 033403 (2011).
[45] O. Hod, J. Chem. Theory Comput. **8**, 1360 (2012).